e-ISSN: 2550-164X

Journal of Mechanical Engineering 22(2) 2025, 15 – 30.

Journal of Mechanical Engineering

Designing of Prediction Model for Parameter Optimization in CNC Machining Based on Artificial Neural Network

Armansyah[1]*, Muhammad Nurul Puji[2], Muhammad Destri Mardhani[1], I Putu Eka Suartana[1], Desmawati[1], Ferdyanto[1], Muhammad Afiff Kusumah[1], Muhammad Umar Yafi[1], Juri Saedon[3]

[1]*Faculty of Engineering, Universitas Pembangunan Nasional Veteran, Jakarta 12450, Indonesia,*
[2]*Automotive and Robotics Engineering Program, Computer Engineering Department BINUS ASO School of Engineering, Bina Nusantara University, Jakarta, Indonesia,*
[3]*School of Mechanical Engineering, Engineering College, Universiti Teknologi MARA (UiTM), Shah Alam 40450, Malaysia*

ARTICLE INFO

Article history:
Received 26 October 2024
Revised 4 February 2025
Accepted 22 February 2025
Online first
Published 31 May 2025

Keywords:
CNC machining
Surface roughness
Extended full factorial design
Artificial Neural Network (ANN)
Normalized Root Mean Squared Error (NRMSE)

DOI:
https://doi.org/10.24191/jmeche.v22i2.4981

ABSTRACT

The consistent surface finishes in polishing remain a significant challenge. Variations in machining parameters often lead to inconsistent results, negatively impacting both the appearance and functionality of polished components. Despite advances in CNC technology, the selection of optimal machining parameters remains complex due to the interplay of multiple factors. This study addresses this gap by developing a prediction model to systematically determine appropriate machining parameters such as cutting speed (v_c), feed rate (v_f), and depth of cut (d_{oc}). Surface roughness (R_a) was used as the key metric to evaluate the surface quality of CNC end-mill products. The above machining parameters were varied according to a 3^3-extended full factorial design, resulting in 108 experimental output targets of R_a. These outputs were then utilized to train an ANN prediction model based on a feed-forward backpropagation (FFBP) algorithm. The results demonstrated a strong correlation coefficient (R = 0.992) across all data sets. In the regression plot, the predicted values closely matched the actual values, indicating a high level of accuracy in the regression model. Furthermore, error evaluation using normalized root mean square error (NRMSE) revealed a low error rate of 3.79%, which is considered highly acceptable, particularly in the context of polishing.

INTRODUCTION

The ongoing advancements in computer numerical control (CNC) machining technology require processes that are both efficient and precise, emphasizing sensitivity and accuracy to enhance product quality. Surface roughness (R_a) is a critical parameter in evaluating the quality of CNC-machined components, as it directly reflects surface morphology and machining performance (Prakashrao Patil et al., 2023; Bonţiu Pop, 2015;

[1*] Corresponding author. *E-mail address*: armansyah@upnvj.ac.id
https://doi.org/10.24191/jmeche.v22i2.4981

Ali et al., 2019; Yahul & Saravanan, 2023; Armansyah et al., 2023). Surface roughness is primarily influenced by deviations at the interface between the tool and workpiece, resulting in varying surface profiles (Alharthi et al., 2017; Sulaiman et al., 2022). Hence, selecting optimal machining parameters is crucial for achieving superior surface finishes and ensuring the functionality of the final product (Khatai et al., 2022). Aluminium alloys, particularly Al 6061, were chosen as the material for this study due to their extensive industrial applications, including automotive, aerospace, and manufacturing. Aluminium alloys are widely utilized for producing lightweight and high-performance components such as parts, Molds, and dies (Abban et al., 2023). Their exceptional machinability, corrosion resistance, and mechanical properties make them ideal for studying the relationship between machining parameters and surface roughness. Furthermore, Aluminium alloys exhibit a high sensitivity to machining conditions, such as cutting speed (v_c), feed rate (v_f), and depth of cut (d_{oc}). This sensitivity makes them particularly suited for evaluating surface roughness and training predictive models.

The advantages of using Aluminium alloys for this study are multifold:

(i) High machinability: Aluminium alloys, especially Al 6061, allow for precise material removal and consistent machining behaviour, ensuring accurate data collection for predictive modelling.
(ii) Sensitivity to parameters: Aluminium's response to machining conditions ensures measurable and reliable variations in surface roughness, which are crucial for developing robust prediction models.
(iii) Industrial relevance: Aluminium alloys are commonly used in manufacturing industries, and optimizing their machining parameters provides practical benefits, making the research outcomes widely applicable.
(iv) Cost-effectiveness: Aluminium is readily available and relatively affordable, enabling cost-efficient experimentation and data generation.
(v) Predictive modelling suitability: The uniformity and predictability of Aluminium alloys minimize external variability, enhancing the accuracy of artificial neural network (ANN) predictions.

Previous studies, focusing on the influence of milling conditions on Aluminium alloys, highlight that R_a is mainly affected by v_c and v_f (Nowakowski et al., 2022; Lazkano et al., 2022; Phokobye et al., 2022). Insufficient parameter settings can lead to poor surface quality, reducing the functionality and reliability of machined components. Consequently, continuous improvement is essential to ensure effective and efficient machining processes while maintaining product quality. However, such improvements often require significant time and cost for experimental work, testing, and validation.

The advent of Industry 4.0 has introduced the need for intelligent manufacturing processes that produce high-quality products efficiently. Artificial intelligence (AI) presents a promising alternative to traditional experimental approaches for optimizing machining processes. By leveraging large datasets, machine learning (ML) models can predict future process outcomes, such as surface roughness in CNC machining. These models utilize statistical techniques to identify patterns in data, enabling the prediction of target outputs based on input parameters.

Machine learning models can learn the underlying structure of data, offering flexibility for tasks such as data augmentation or generating synthetic training data. Additionally, these models improve over time as they process more data, allowing for continuous learning and adaptation to changing conditions (Wang et al., 2018). Supervised and unsupervised learning are two fundamental types of machine learning, each serving different objectives. Supervised learning involves training a model on labeled data, where each input is paired with a known output, allowing the model to make predictions. In contrast, unsupervised learning analyzes unlabeled data to detect patterns, relationships, or structures without predefined outputs (Wang et al., 2021). Both techniques offer powerful solutions to a wide range of engineering challenges (Bharot et al., 2024; Narwane et al., 2023; De Oliveira Santos & Schneider Hahn, 2023).

https://doi.org/10.24191/jmeche.v22i2.4981

To overcome the challenges of optimizing machining parameters without depending exclusively on costly experimental approaches, this study utilizes an ANN. Modeled after the neural architecture of the human brain, ANNs comprise multiple interconnected layers, including input, hidden, and output layers. These networks use algorithms such as feed-forward backpropagation (FFBP) to train models by adjusting weights (w_{ij}) and biases (b_j) (Zou et al., 2008; Bayraktar & Alparslan, 2022). It is constructed in such a way as a causal relation between variables or process parameters affecting the corresponding results. The ANN model can determine the output target generated by the selected input. Mathematically, it describes a structural model of the network as the function f of x to y (f: $x \rightarrow y$). It is interconnected with layers consisting of an input layer, an output layer, and one or more hidden layers interconnected with nodes as neurons (Armansyah et al., 2020). The data flows in the structure of the network via the FFBP algorithm. They are trained and learn the process of parameter values, w_{ij} and b_j (Fischer & Igel, 2014). Technically, the process of learning starts in the forward propagation stage to train the data throughout the model structure via w_{ij} and b_j. At the end of the structure, the output layer predicts the output target and estimates the error. It was done through gradient descent FFBP learning procedures to reduce the mean squared error (MSE) (Mouloodi et al., 2022).

A new study on laser-assisted turning of NITINOL shape memory (Naresh et al., 2024) used the ANN technique to optimize the CNC turning process in various machining conditions using the ANN with the BP algorithm. Another similar study has been done (Erkaymaz, 2020), who developed a Newman–Watts small-world feed-forward artificial neural network for better classification and prediction performance instead of conventional feed-forward artificial neural networks. Another effort in the FF-BPNN algorithm had been successfully performed (Murugesan et al., 2019) to predict the hot deformation behaviour of medium carbon steel material. A study to predict the output target of welding strength in Al 6061 by employing an ANN based on input data of process parameters was performed (Chavan & Shete, 2015). The serial numbers of experiments are performed using full factorial designs 3^3 to evaluate the impact of R_a from the combination of the main parameters. It was obtained that the MSE predicted performance showed an average error of 15.35 %. Another study by (Armansyah et al., 2020) used FFBP ANN algorithm to optimize process variables in friction stir spot welded (FSSW) in Aluminium alloy, via plunge depth and dwell time, through 27 experiments, and evaluated mechanically using tensile shearing load testing. It can be seen that the FFBP-ANN algorithm provided relatively good predictions since the correlation coefficient relatively (R) close to 1.

Based on these studies, it is evident that the selection and combination of machining parameters significantly influence the final surface quality, measured by R_a. This study investigates the effect of three process parameters v_c, v_f, and d_{oc}, on R_a. A predictive model using ANNs with the FFBP algorithm is then developed to optimize these parameters, providing a cost-effective and efficient solution for CNC machining process optimization.

MATERIAL AND METHOD

Before developing the prediction model via ANNs, the Aluminium alloy block of Al-6061 was prepared to produce a workpiece sample for the experiment in the CNC milling. The Aluminium alloy block of Al-6061 was set with a geometry of 300 x 300 x 100 mm as shown in Fig 1.

A 3-axis high-speed computer numerical control machine (HSM) of LG-1000 HARTFORD, which is available in the manufacturing laboratory at the Engineering Faculty Universitas Pembangunan Nasional Veteran Jakarta, was employed to conduct machining using an end mill cutter utilized in dry cutting conditions. The experimental design contained variations of three factors at three levels based on an extended full factorial design (3^3) as shown in Table 1.

https://doi.org/10.24191/jmeche.v22i2.4981

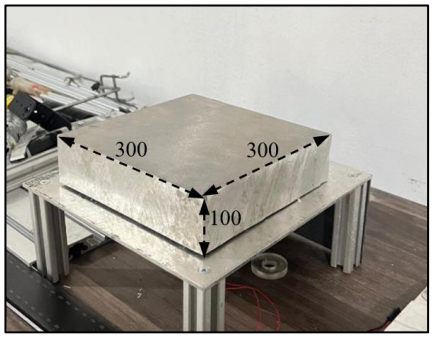

Fig. 1. The geometry of the Aluminum block of Al-6061 with long (*l*), width (*w*), and thickness (*t*) of 300 mm, 300 mm, and 100 mm, respectively.

Table 1. The range of selected parameters in this study is represented by three factors of v_c, v_f, and d_{oc} with respect to three levels of low-, middle-, and high-level parameter variations

Level	Low	Middle	High
v_c (rpm)	160	900	1650
v_f (mm/min)	110	160	210
d_{oc} (mm)	0.1	0.3	0.5

Through these parameter variations, the finished cutting of the sample specimens were measured randomly for R_a as the output responses at three different locations located on the workpiece surface along the cutting path using a surface roughness tester of Surfcoder SE300. The measurement was done by attaching the sensor from the measuring tool of the surface roughness tester to the point at 3 different locations on the workpiece randomly along the cutting path. This produced 27 measurements of R_a from 27 parameters variations as the output responses including as data input for development of the ANNs prediction model.

Evaluation of the surface quality of the end-mill products was performed through the R_a measurements at each experiment of CNC milling via selected parameters variation according to Table 1. Each experiment applied in the CNC milling, is connected to the 27 parameter variations based on the full factorial design of the experiment (3^3). The random R_a measurements were done on several locations on machining surfaces at each experiment (run) using a surface roughness measuring instrument of SE300. In total, there were 108 R_a measurements were done from all locations of machining surfaces. Fig 2 describes R_a measurements along the machining surfaces.

The structure of the ANN network (Fig 3) was developed with one input layer containing three neurons of three input parameters i.e. v_c, v_f, and d_{oc}. In the output layer, one neuron was seated up corresponding to R_a. A hidden layer was managed. The 27 set of parameter variation as the input patterns, with four repetitions measurement on the machining surfaces at each set randomly, are fed into the network structure via the FFBP algorithm in the Matlab environment for training (70%), testing (15%), and validating (15%).

The mean square error (MSE) is a statistical metric that quantifies the average squared deviation between observed values and predicted values in regression analysis. In this study, the average square of error is measured between data from actual R_a measurements and the R_a from the developed ANN model. It is a common measure of the quality of an estimator—it tells you how close a regression line is to a set of points. It is defined by the formula MSE the following (Swamidass, 2000),

https://doi.org/10.24191/jmeche.v22i2.4981

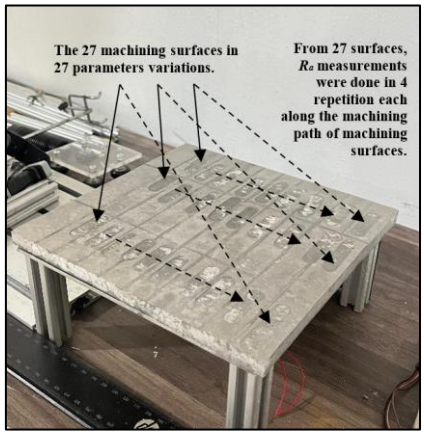

Fig. 2. The R_a measurements were done at 27 machining surfaces with four repetitions along the machining paths.

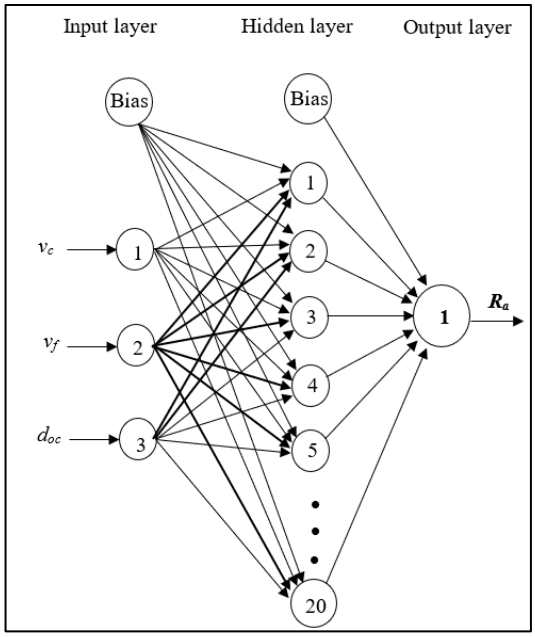

Fig. 3. Topology of surface roughness's (R_a) ANNs prediction model.

$$MSE = \frac{1}{n}\sum_{i=1}^{n}(y_i - \hat{y}_i)^2 \quad (1)$$

where n is the number of data points (R_a measurements), y_i is the output for the *i-th* data point, and $\hat{y}_i$ is the predicted value of the *i-th* data point. Subsequently, the aggregate the magnitudes of the errors served by the root means square error (RMSE) in predictions to a certain of times. RMSE is especially valuable for evaluating and comparing the performance of different models on the same dataset, as it quantifies how accurately each model predicts the target variable (Hyndman & Koehler, 2006). Below is **t**he RMSE formula,

https://doi.org/10.24191/jmeche.v22i2.4981

$$RMSE = \sqrt{MSE} = \sqrt{\frac{1}{n}\sum_{i=1}^{n}(y_i - \hat{y}_i)^2} \quad (2)$$

where the of $y_{max} - y_{min}$ is described as the highest of measured data minus the lowest of the measured data. Ultimately, the normalizing root mean square error (NRMSE) was employed to evaluate data sets with different ranges in percentage. The lower the NRMSE, the less error variance will be obtained (Kobayashi, Kazuhiko & Salam, 2000).

$$NRMSE = \frac{RMSE}{\bar{y}}\frac{RMSE}{y_{max} - y_{min}} = \frac{\sqrt{\frac{1}{n}\sum_{i=1}^{n}(y_i - \hat{y}_i)^2}}{y_{max} - y_{min}} \quad (3)$$

The Levenberg-Marquardt (LM) is adopted into FFBP to find the parameters that minimize the sum of the squares of differences between observed and predicted values from a nonlinear model. Trainlm is used in LM training algorithm to adjust the parameters (weights and biases) of the neural network model such that the difference between predicted and actual outputs (the error or loss) is minimized. Additionally, to normalize and balance the activation patterns of neurons, the hyperbolic tangent sigmoid transfer function (tansig) and the linear transfer function (purelin) are employed in FFBP ANN for pattern recognition and fitting tasks, respectively. The details of the FFBP ANN algorithm are provided in Table 2.

Table 2. FFBP specification in the neural network

Type	Feedforward backpropagation (FFBP)
Algorithm	Levenberg-Marquardt (LM)
Training function	Trainlm
Adaption learning function	Learngdm
Transfer function	Tangent sigmoid (Tansig), linear (Purelin)
Number of layers; data ratio	3 input and 1 output; 70:15:15
Number of hidden layer; neurons	1; 20

The procedure of the FFBP network in the ANN prediction model is explained in the following and described in Fig 4:

(i) Define network structure and set the three input process parameters for CNC-machining (v_c, v_f, and d_{oc}),
(ii) Determine the output target as the actual R_a,
(iii) Initialize the ANN model,
(iv) Feed the data input into the network,
(v) Perform forward-propagation for the data input via neurons throughout layers in the network and multiply with the w_{ij} and b_j,
(vi) Check the error between the predicted target with the actual target,
(vii) Back-propagation starts to propagate the data to the parameters in the model of the neural network,
(viii) Update each parameter using its gradient to move it in the direction that reduces the loss function,
(ix) Iterate the previous steps by multiple epochs or until the convergence criteria are met, and consider the ANN model is good.
(x) Start the simulation of the ANN model.

https://doi.org/10.24191/jmeche.v22i2.4981

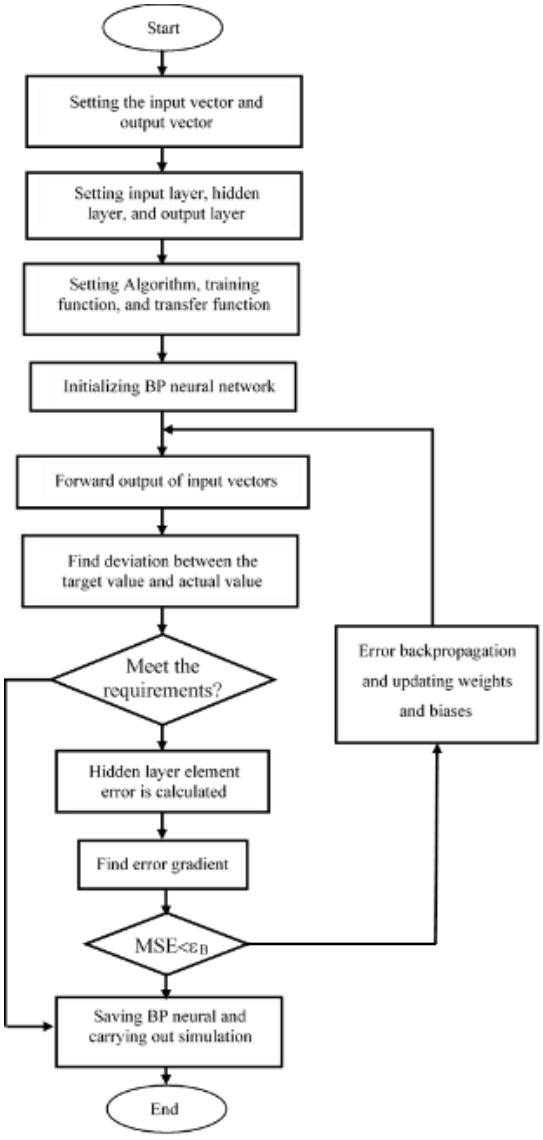

Fig. 4. The procedure of FFBP algorithm in ANN network model.

RESULTS

In this stage, an ANN model was used to develop a predictive model for R_a in CNC machining. These predicted R_a can be traced based on 27 variations of 3 input parameters with 3 levels, and with four repetitions randomly at each variation, producing 108 output target R_a fed into the ANNs prediction model. A detailed result of 27 variations of the TSL Test with 108 output targets R_a can be seen in Table 3.

https://doi.org/10.24191/jmeche.v22i2.4981

Table 3. The total of 243 measurements of surface roughness (R_a) based on four repetitions affected by selected parameters through the CNC milling process at each run.

Exp.	v_c (rpm)	v_f (mm/min)	d_{oc} (mm)	Surface Roughness (R_a) measurements on the surfaces at each experiment			
				1st location (μm)	2nd location (μm)	3rd location (μm)	4th location (μm)
1	160	110	0.1	0.34	0.38	0.35	0.39
2	160	160	0.3	0.40	0.47	0.45	0.48
3	160	210	0.5	0.47	0.44	0.45	0.43
4	900	110	0.1	0.57	0.64	0.62	0.65
5	900	160	0.3	0.65	0.71	0.68	0.67
6	900	210	0.5	0.71	0.69	0.74	0.72
7	1650	110	0.1	0.86	0.81	0.85	0.82
8	1650	160	0.3	0.90	0.85	0.88	0.91
9	1650	210	0.5	0.99	0.94	0.92	0.95
10	160	110	0.1	0.47	0.50	0.52	0.53
11	160	160	0.3	0.56	0.62	0.54	0.58
12	160	210	0.5	0.55	0.59	0.57	0.56
13	900	110	0.1	0.72	0.77	0.71	0.73
14	900	160	0.3	0.78	0.82	0.76	0.79
15	900	210	0.5	0.85	0.82	0.81	0.89
16	1650	110	0.1	0.89	0.94	0.88	0.96
17	1650	160	0.3	1.03	1.00	0.97	1.02
18	1650	210	0.1	0.61	0.60	0.62	0.67
19	160	110	0.3	0.67	0.71	0.70	0.68
20	160	160	0.5	0.72	0.79	0.73	0.80
21	160	210	0.1	0.79	0.84	0.82	0.86
22	900	110	0.3	0.86	0.91	0.85	0.89
23	900	160	0.5	0.98	0.91	0.94	0.99
24	900	210	0.1	1.15	1.13	1.09	1.07
25	1650	110	0.3	1.08	1.12	1.09	1.13
26	1650	160	0.5	1.14	1.13	1.17	1.18
27	1650	210	0.1	0.34	0.38	0.35	0.39

Regression Plot

Fig 5 describes a regression plot that shows the relationship between predicted values (output of the neural network model) and actual output target (from R_a measurement) for all patterns across training, validation, and testing sets in a prediction model related to CNC machining. The *x*-axis represents the actual output target (R_a measurements), and the *y*-axis shows the predicted output target (performed in ANN model). Ideal line (diagonal line) where all points would lie perfectly on a diagonal line. This would mean that the predicted values exactly match the actual experimental values. Trend line or regression line was plotted to show the overall relationship between predicted and actual values. This line helps visualize how well the model's predictions align with the actual data. A good model will have points clustered closely around this line.

Based on the result obtained, it can be seen that the regression plot for ANN prediction model is showing very promising results. In the training set, the correlation coefficient (*R*) was 0.992, indicating a very strong positive linear relationship between the predicted values and the actual experimental values. A value close to 1 suggests that the model's predictions closely match the actual data points in the training set. The *R* in the testing set was 0.989. This is slightly lower than the training set but still very high, indicating that the model generalizes well to unseen data. The high *R*-value suggests that the predictions on the testing set are also closely aligned with the actual experimental values. Meanwhile, the *R* was 0.995 for the validation set. This is even higher than both the training and testing sets, which indicates that the model performs exceptionally well on the validation data. The validation set's high *R*-value suggests that the model is robust and consistent in its predictions across different subsets of data. The overall *R* for all data sets combined is 0.992. This indicates that when considering all the data together (training, testing, and

https://doi.org/10.24191/jmeche.v22i2.4981

validation sets), the ANN prediction model maintains a high level of accuracy and consistency in its predictions across the entire dataset.

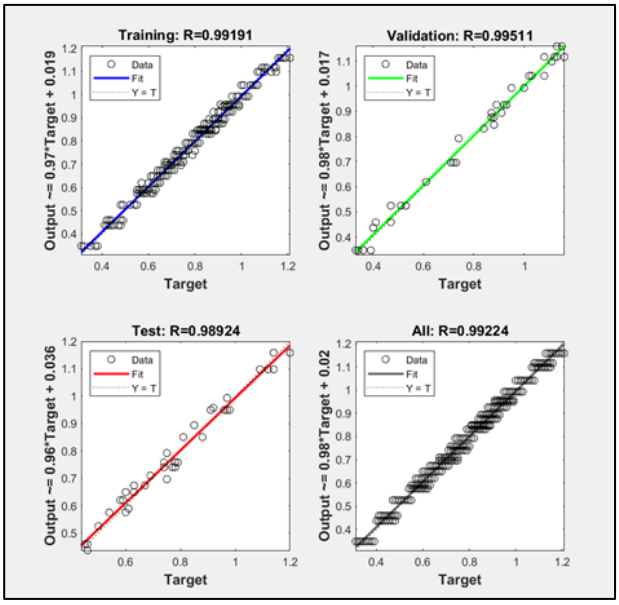

Fig. 5. Pattern for training, validation, and testing of ANN prediction model via regression plot.

Error Deviation

With regard to the technique of determining the error (MSE) of the 108-output targets of R_a between actual values and ANNs (predicted) values can be seen partly in Table 4.

Table 4. The calculation of error values between actual values and the ANN

Number of locations at each experiment	R_a Actual (y_i) in µm	R_a ANNs $(\hat{y}_i)$ in µm	Error $(y_i - \hat{y}_i)$ in µm	Error^2 $(y_i - \hat{y}_i)^2$ in µm
1	0.34	0.36582	-0.02582	0.00067
2	0.38	0.36582	0.01418	0.0002
3	0.35	0.36582	-0.01582	0.0003
4	0.39	0.36582	0.02418	0.0004
5	0.4	0.44056	-0.04056	0.0016
6	0.47	0.44056	0.02945	0.0009
…	…	…	…	…
103	1.09	1.12212	-0.032129	0.001032
104	1.13	1.12213	0.007871	0.000062
105	1.14	1.16708	-0.027083	0.000734
106	1.13	1.16708	-0.037083	0.001375
107	1.17	1.16708	0.002917	0.000009
108	1.18	1.16708	0.012917	0.000167
			$\sum_{i=1}^{n}(y_i - \hat{y}_i)^2$ = where n=108	0.109839

https://doi.org/10.24191/jmeche.v22i2.4981

Based on the 108-output target, the NRMSE can be calculated as follow:

$$MSE = \frac{1}{n}\sum_{i=1}^{n}(y_i - \hat{y}_i)^2 = \frac{1}{108}\sum_{i=1}^{108}(y_i - \hat{y}_i)^2 = \frac{1}{108}(0.109839) = 0.00101703$$

$$RMSE = \sqrt{MSE} = \sqrt{0.00101703} = 0.03189095$$

$$NRMSE = \frac{RMSE}{y_{max} - y_{min}} = \frac{0.03189095}{1.18 - 0.34} = 0.03796541$$

$$= 0.03796541 \times 100\% = 3.79\ \%$$

Based on the calculation of NRMSE above, this ANNs prediction model is nearer to the actual values with 3.79% deviation of error for all patterns. It revealed that the error is good to acceptable justification.

Simulation The Predicted ANN Model

In this study, the FFBP ANN algorithm was implemented in the MATLAB environment to model the predicted R_a value based on the process parameters of v_c, v_f, and d_{oc} in CNC machining. The three-dimensional plots of the predicted R_a were built based on two varied v_c and v_f at constant d_{oc}. Fig 6 defines predicted R_a according to the v_c and v_f with a correlation of d_{oc} at 0.1 mm. It is revealed that the setting with lower v_c and lower v_f represents a dark blue region indicating the lower surface roughness R_a. A picked sample of lower R_a is represented by 0.38 µm at 104 mm/minutes of v_f and 193 rpm of v_c. The predicted R_a is continuously increased sharply (in the bright blue region) with continuous increases of v_c and v_f simultaneously as can be seen at v_f of about 214 mm/minutes and v_c of about 187 rpm obtained R_a of about 0.647 µm. Subsequently, the R_a continues to reach a higher value in the yellow region, with increasing v_f and v_c, producing R_a with about 1.08 µm at v_f of about 215 mm/minutes and v_c of about 1644 rpm. The results show that the predicted R_a increases notably as v_f and v_c increase.

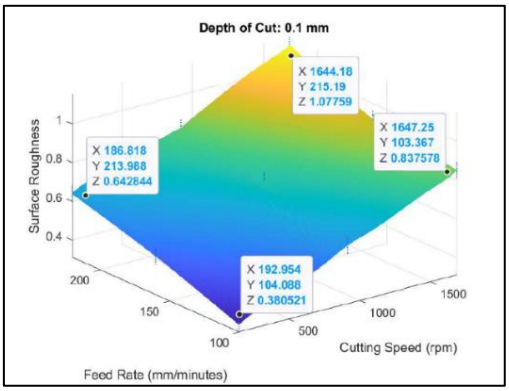

Fig. 6. The combined effect of v_c and v_f on R_a at d_{oc} 0.1 mm.

Meanwhile, Fig 7 shows the relationship between v_c and v_f that affected the R_a at 0.3 mm of d_{oc}. The dark blue region represents the low surface roughness R_a of about 0.48 µm as v_c at about 196 rpm and v_f at about 106 mm/minute. In the light blue region, the R_a increases gradually when v_c and v_f increase with many options of both combinations. As described in Fig 10, the moderate R_a of around 0.7 µm to 0.8 µm can be found by controlling the lower or higher v_c combined with v_f, and vice versa. The highest value of R_a reached

https://doi.org/10.24191/jmeche.v22i2.4981

around 1.1 μm (in the yellow region) with the highest value of v_c and v_f (up to maximum values). It confirmed that the R_a increased gradually together with increasing the v_c and v_f at constant d_{oc}.

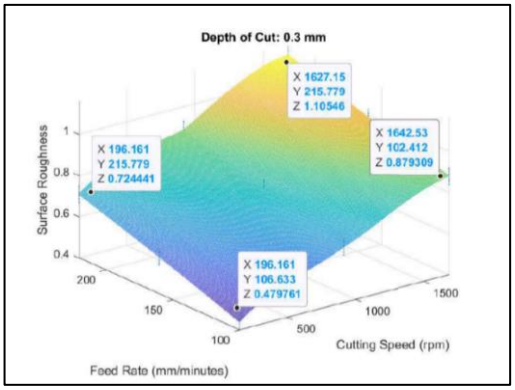

Fig. 7. The combined effect of v_c and v_f on R_a at d_{oc} 0.3 mm.

Fig 8 displays the intention of v_c and v_f that affected the R_a at 0.5 mm of d_{oc}. Similar figures as depicted in Fig 6 and Fig 7, Fig 8 also shows the lower R_a at about 0.5 μm located in the dark blue region obtained by using lower v_c and v_f of about 196 rpm and about 103 mm/minutes respectively. The R_a's increasing in the light blue region of about 0.76 μm and 0.95 μm when controlling the lower or higher v_c combined with v_f. Then, *Ra*'s reach higher numbers of about 1.16 μm in the yellow region, together with the increase of v_c and v_f up to maximum values.

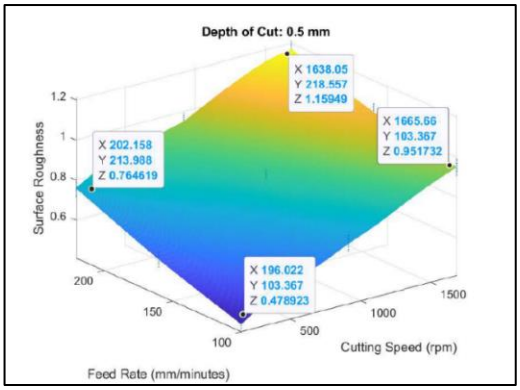

Fig. 8. The combined effect of v_c and v_f on R_a at d_{oc} 0.5 mm.

To validate the developed ANNs model, additional run-tests are performed using random configuration of v_c, v_f, and d_{oc} as shown in Table 5. The results from each run-test yield actual R_a measured in three locations at each path of the run-test. The Table shows the comparison of R_a between Actual and ANNs confirmed closer to each other, with the error between 0.6% - 1.05% along the nine-run tests with low deviation and errors as depicted in Fig 9. This graphical representation (Fig 9) is presented to serve those comparisons between R_a (actuals and ANNs) including a deviation of errors. Those actual R_a results produced errors NRMSE (4.12%) via MSE and RMSE. It can be seen that the deviation of error between about 0.699% – 1.050% which is good to acceptable justification of 4.12% error from the calculation of the normalize root mean squared error (NRMSE).

https://doi.org/10.24191/jmeche.v22i2.4981

Table 5. Additional run-tests using random configuration of v_c, v_f, and d_{oc} to validate predicted R_a values from ANNs model

Run	Random Configurations			R_a -actual in µm	R_a – ANNs in µm	Error $(y_i - \hat{y}_i)$ in µm	Error^2 $(y_i - \hat{y}_i)^2$ in µm	Error (%)
	v_c (rpm)	v_f (mm/min)	d_{oc} (mm)					
				0.805	0.811	-0.006	0.000036	0.805
28	1579	107	0.1	0.801	0.811	-0.099	0.000098	0.801
				0.805	0.811	-0.006	0.000036	0.805
				0.699	0.707	-0.008	0.000064	0.699
29	188	215	0.3	0.701	0.707	-0.006	0.000036	0.701
				0.699	0.707	-0.008	0.000064	0.699
				1.050	1.058	-0.008	0.000064	1.050
30	1611	202	0.5	1.030	1.058	-0.028	0.000784	1.030
				0.999	1.058	-0.059	0.003481	0.999
						$\sum_{i=1}^{n}(y_i - \hat{y}_i)^2$ = where n=9	0.004663	

The NRMSE can be calculated as follow:

$$MSE = \frac{1}{n}\sum_{i=1}^{n}(y_i - \hat{y}_i)^2 = \frac{1}{9}\sum_{i=1}^{9}(y_i - \hat{y}_i)^2 = \frac{1}{9}\,(0.004663) = 0.000518$$

$$RMSE = \sqrt{MSE} = \sqrt{0.000518} = 0.014457$$

$$NRMSE = \frac{RMSE}{y_{max} - y_{min}} = \frac{0.014457}{1.050 - 0.699} = 0.041187955$$

$$= 0.041187955 \times 100\% = 4.12\%$$

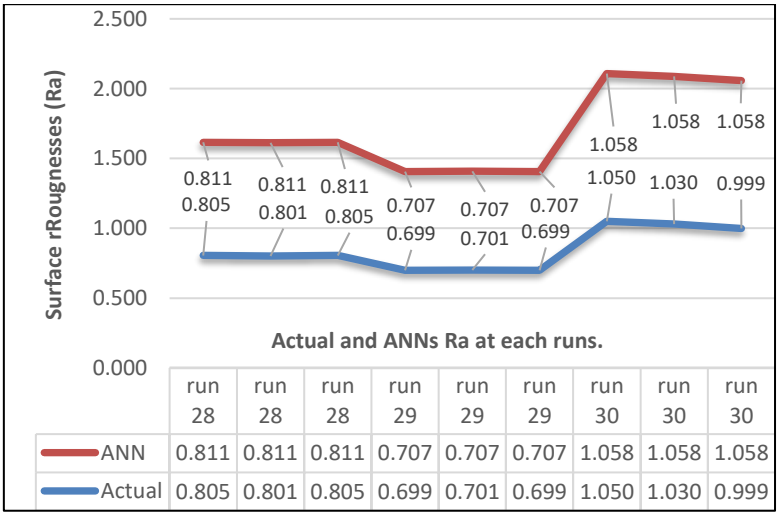

Fig. 9. Comparison of R_a (actuals and ANNs) from run-tests of 28, 29, and 30 each at three repetitions.

Based on the R_a validation above using random parameters (v_c, v_f, and d_{oc}), it can be seen that the percentage of error NRMSE was less than 5% which is close to the actual R_a results done via experiments and measurements.

https://doi.org/10.24191/jmeche.v22i2.4981

DISCUSSION

The ANN-based prediction model developed in this study exhibited excellent accuracy in estimating R_a by considering variations in v_c, v_f, and d_{oc}. The model's reliability is supported by a high correlation coefficient (R = 0.992) and a low normalized root mean squared error (NRMSE = 3.79%). These results align well with previous studies that have utilized ANN for machining process optimization.

Naresh et al. (2024) successfully implemented ANN in laser-assisted turning of NITINOL shape memory alloys using a backpropagation (BP) algorithm. Their model provided accurate predictions of machining performance under varying conditions. Similar to our findings, their study confirmed that ANN-based models significantly reduce prediction errors and improve machining efficiency. Furthermore, Erkaymaz (2020), explored a Newman–Watts small-world feed-forward ANN topology, demonstrating enhanced classification and prediction performance compared to conventional ANN models. This supports our approach of leveraging ANN for CNC machining process optimization.

Another relevant study by Murugesan et al. (2019), employed the FF-BPNN algorithm to predict the hot deformation behavior of medium carbon steel material. Their findings showed that the ANN model could successfully predict material behavior with minimal deviation from actual values. Similarly, (Chavan & Shete, 2015), used ANN to predict the welding strength of Al 6061 based on input process parameters. Their model achieved an acceptable error margin of 15.35%, which is higher than our model's error rate of 3.79%. This indicates that our ANN model provides improved accuracy, likely due to the extended full factorial design used in parameter selection and training.

Moreover, Armansyah (2020), applied the FFBP-ANN algorithm to optimize process variables in FSSW of Aluminium alloys. Their correlation coefficient (R) was close to 1, demonstrating a strong prediction capability similar to our model. These findings reinforce that ANN-based models are effective for optimizing machining parameters in metal processing applications.

Our study further validates findings Nowakowski et al. (2022), who investigated the influence of milling conditions on the surface roughness of Aluminium alloys. Their study highlighted the influence of v_c and v_f on R_a values, consistent with our findings that demonstrate a steady rise in R_a as v_c and v_f increase while maintaining a constant d_{oc}. Additionally, Lazkano et al. (2022), developed roughness maps to determine optimal milling process parameters, which share similarities with our ANN-based approach in identifying the best machining conditions for achieving minimal surface roughness.

In comparison to Phokobye et al. (2022), who studied hardened tool steel during face milling operations, our ANN model achieved a higher prediction accuracy. Their study reported prediction errors of approximately 5%, whereas our model achieved an NRMSE of 3.79%, further demonstrating the effectiveness of our approach.

To ensure the reliability of our findings, additional validation tests were conducted using random configurations of v_c, v_f, and d_{oc}. The results closely matched the actual measurements, with error percentages ranging from 0.6% to 1.05%. These deviations are considerably lower than those reported in previous ANN studies on machining process optimization above.

Overall, the results obtained in this study are in strong agreement with existing literature, confirming that ANN models offer a powerful tool for optimizing CNC machining parameters. Our findings provide a refined approach with reduced error margins and improved accuracy in surface roughness prediction compared to prior research.

https://doi.org/10.24191/jmeche.v22i2.4981

CONCLUSION

This research study delves into the application of AI for enhancing CNC milling, specifically focusing on predicting optimal machining parameters for end-mill products. Using data from CNC machining on Al 6061 workpiece samples, a prediction model was developed using the FFBP algorithm within an ANN. The model was trained, tested, and validated using variations of three machining parameters v_c, v_f, and d_{oc} to predict R_a. The study demonstrated the successful application of an AI-based ANN prediction model for optimizing machining parameters in CNC milling. The model achieved a high correlation coefficient (R = 0.992) and a low normalized root mean squared error (NRMSE=3.79%), confirming its accuracy in predicting R_a. The extended full factorial design yielded reliable results with minimal experimental effort, showcasing the model's potential to enhance efficiency and precision in machining processes, including polishing applications. The findings highlight the potential of AI in industrial machining processes, optimizing them for efficiency and accuracy.

ACKNOWLEDGEMENTS

This work was supported by the "Hibah Internal PKM-T UPN Veteran Jakarta 2024" [052/UN61.4/PkM.PKM-T/2024].

CONFLICT OF INTEREST STATEMENT

All authors declare that they have no conflicts of interest.

AUTHORS' CONTRIBUTIONS

The authors confirm the equal contribution in each part of this work. All authors reviewed and approved the final version of this work.

REFERENCES

Abban, S., Ikumapayi, O. M., Ogedengbe, T. S., Afolalu, S. A., Ananaba, C., & Ogundipe, A. T. (2023). Development of aluminium-tin alloy for high strength application. Materials Today: Proceedings, 2023, 1–5.

Alharthi, N. H., Bingol, S., Abbas, A. T., Ragab, A. E., El-Danaf, E. A., & Alharbi, H. F. (2017). Optimizing cutting conditions and prediction of surface roughness in face milling of AZ61 using regression analysis and artificial neural network. Advances in Materials Science and Engineering, 2017, 7560468.

Ali, M. A., Ishfaq, K., & Jawad, M. (2019). Evaluation of surface quality and mechanical properties of squeeze casted AA2026 Aluminum alloy using response surface methodology. The International Journal of Advanced Manufacturing Technology, 103, 4041–4054.

Armansyah. (2020). Friction stir spot welded characterization of aluminium alloy 5052-H112 and prediction model using artificial neural network. [Doctoral dissertation, Universiti Teknologi MARA].

https://doi.org/10.24191/jmeche.v22i2.4981

Retrieved from https://ir.uitm.edu.my/id/eprint/32514/.

Armansyah, Chie, H. H., Saedon, J., & Adenan, S. (2020). Feed-forward back-propagation (FFBP) algorithm for property prediction in friction stir spot welding of aluminium alloy. IOP Conference Series: Earth and Environmental Science, 426, 012128.

Armansyah, Zulaihah, L., Nasution, S. R., Sinaga, G. G., Saedon, J., & Sudianto, A. (2023). Design parameters optimization in CNC machining based on Taguchi, ANOVA, and screening method. Journal of Mechanical Engineering, 12, 209–224.

Bayraktar, Ş., & Alparslan, C. (2022). Artificial neural networks for machining. In K. K. Gajrani, A. Prasad & A. Kumar (Eds.), Advances in Sustainable Machining and Manufacturing Processes (pp.189-204). CRC Press.

Bharot, N., Verma, P., Soderi, M., & Breslin, J. G. (2024). DQ-DeepLearn: Data quality driven deep learning approach for enhanced predictive maintenance in smart manufacturing. Procedia Computer Science, 232, 574–583.

Bonţiu Pop, A. B. (2015). Application of Taguchi's method for study of machining parameters on surface roughness of 7136 aluminum alloy in end milling. Applied Mechanics and Materials, 809–810, 123–128.

Chavan, A., & Shete, M. T. (2015). Optimization of friction stir spot welding process using artificial neural network. International Journal of Science Technology & Engineering, 1(10), 353-358.

De Oliveira Santos, F., & Schneider Hahn, I. (2023). A systematic literature review and taxonomy proposition of machine learning techniques in smart manufacturing. Multidisciplinary Business Review, 16(2), 66–88.

Erkaymaz, O. (2020). Resilient back-propagation approach in small-world feed-forward neural network topology based on Newman–Watts algorithm. Neural Computing and Applications, 32, 16279–16289.

Fischer, A., & Igel, C. (2014). Training restricted Boltzmann machines: An introduction. Pattern Recognition, 47(1), 25–39.

Hyndman, R. J., & Koehler, A. B. (2006). Another look at measures of forecast accuracy. International Journal of Forecasting, 22(4), 679–688.

Khatai, S., Kumar, R., Sahoo, A. K., & Panda, A. (2022). Investigation on tool wear and chip morphology in hard turning of EN 31 steel using AlTiN-PVD coated carbide cutting tool. Materials Today: Proceedings, 59(3), 1810–1816.

Kobayashi, K., & Salam, M. U. (2000). Comparing simulated and measured values using mean squared deviation and its components. Agronomy Journal, 92(2), 345–352.

Lazkano, X., Aristimuño, P. X., Aizpuru, O., & Arrazola, P. J. (2022). Roughness maps to determine the optimum process window parameters in face milling. International Journal of Mechanical Sciences, 221, 107191.

Mouloodi, S., Rahmanpanah, H., Gohery, S., Burvill, C., & Davies, H. M. S. (2022). Feedforward backpropagation artificial neural networks for predicting mechanical responses in complex nonlinear structures: A study on a long bone. Journal of the Mechanical Behavior of Biomedical Materials, 128, 105079.

Murugesan, M., Sajjad, M., & Jung, D. W. (2019). Hybrid machine learning optimization approach to

https://doi.org/10.24191/jmeche.v22i2.4981

predict hot deformation behavior of medium carbon steel material. Metals, 9(12), 1315.

Naresh, C., Sameer, M. D., & Bose, P. S. C. (2024). Comparative analysis of RSM, ANN and ANFIS techniques in optimization of process parameters in laser assisted turning of NITINOL shape memory alloy. Lasers in Manufacturing and Materials Processing, 11, 371–401.

Narwane, V. S., Gunasekaran, A., Gardas, B. B., & Sirisomboonsuk, P. (2023). Quantum machine learning a new frontier in smart manufacturing: a systematic literature review from period 1995 to 2021. International Journal of Computer Integrated Manufacturing, 38(1), 116–135.

Nowakowski, L., Bartoszuk, M., Skrzyniarz, M., Blasiak, S., & Vasileva, D. (2022). Influence of the milling conditions of aluminium alloy 2017A on the surface roughness. Materials, 15(10), 3626.

Phokobye, S., Desai, D., Tlhabadira, I., Sadiku, R., & Daniyan, I. (2022). Investigating the surface roughness of hardened tool steel (2379) during face milling operation. International Journal of Mechanical Engineering and Robotics Research, 11(1), 22–30.

Prakashrao Patil, S., Leela Prasad, G., Sai Kiran, C., Kumar, S., Ramasamy, V., & Mohammed Ali, H. (2023). Surface roughness and topography of EDM machining of Inconel 718. Materials Today: Proceedings, 2023, 1–6.

Sulaiman, S., Alajmi, M. S., Wan Isahak, W. N., Yusuf, M., & Sayuti, M. (2022). Dry milling machining: optimization of cutting parameters affecting surface roughness of aluminum 6061 using the Taguchi method. International Journal of Technology, 13(1), 58-68.

Swamidass, P. M. (2000). Mean Squared Deviation (MSD) Error. Encyclopedia of Production and Manufacturing Management (p. 463). Springer New York.

Wang, J., Ma, Y., Zhang, L., Gao, R. X., & Wu, D. (2018). Deep learning for smart manufacturing: Methods and applications. Journal of Manufacturing Systems, 48(C), 144–156.

Wang, L., Mykityshyn, A., Johnson, C. M., & Marple, B. D. (2021). Deep learning for flight demand and delays forecasting. American Institute of Aeronautics and Astronautics (AIAA) Aviation 2021 Forum (pp. 1-11). American Institute of Aeronautics and Astronautics, Inc.

Yahul, M., & Saravanan, R. (2023). An analysis on CNC machined surface roughness between AA7475 and AA7475/fly ash composite. Journal of Physics: Conference Series (p. 012026). IOP Publishing Ltd.

Zou, J., Han, Y., & So, S. S. (2008). Overview of Artificial Neural Networks, In D. J. Livingstone (Ed.), Artificial Neural Networks (pp. 14–22). Humana Press.

https://doi.org/10.24191/jmeche.v22i2.4981